JOURNAL OF MATERIALS SCIENCE 17 (1982) 2503–2513

Direct current electrical conductivity of gamma ferric oxide

A. K. NIKUMBH, K. S. RANE, A. J. MUKHEDKAR
University Department of Chemistry, Ganeshkhind, Pune – 411 007, India

The study of the direct current electrical conductivity, σ, of freshly prepared γ-Fe_2O_3 and that of a sample stored for seven days in static air suggests that γ-Fe_2O_3 adsorbs oxygen and water from the atmosphere. From infra-red spectra it is deduced that the absorbed water in γ-Fe_2O_3 is present as the physically adsorbed water and as lattice water. The adsorbed oxygen and physically adsorbed water are removed by heating to 100° C, while the lattice water remains in γ-Fe_2O_3 even up to 280° C. The removal of lattice water is associated with a decomposition during which some of the hydrogen formed occupies the vacancy sites. This suggested formation of the hydrogen ferrite phase is based on the kink in the log σ against T^{-1} curve observed at 177° C. This kink is very well resolved for a sample equilibrated at 100° C in normal atmosphere, and the measurements of σ above 100° C of this sample are done in an N_2 atmosphere. The suggestion that the hydrogen ferrite phase is formed has been substantiated by comparison of the X-ray diffraction patterns of γ-Fe_2O_3 heated under the different atmospheres. From the log σ against T^{-1} plot for a sample heated under a nitrogen atmosphere the activation energy is small (< 0.05 eV) up to 215° C, and it is comparatively large (0.95 eV) above 215° C. These results suggest a hopping mechanism for the direct current electrical conductivity of γ-Fe_2O_3. This suggestion has been substantiated by data of the temperature variation of Seebeck voltage.

1. Introduction

While determining the experimental conditions for the synthesis of γ-Fe_2O_3 from $FeC_2O_4 \cdot 2H_2O$ in static air containing a known percentage of water vapour, a type of hysteresis was observed in the log σ against T^{-1} plot (σ being the direct current electrical conductivity) of the freshly prepared γ-Fe_2O_3 during the heating and cooling cycles [1]. This paper reports a detailed analysis of this type of behaviour.

2. Experimental procedure

The procedures used for the measurements of direct current electrical conductivity, infra-red spectra, X-ray diffraction patterns and magnetic properties were similar to that reported earlier [1]. The thermal analyses were done on a MOM Derivatigraph. The synthesis of γ-Fe_2O_3 by the solid state decomposition of $FeC_2O_4 \cdot 2H_2O$ has also been given earlier [1]. The details of the measurements of Seebeck voltage and of synthesis of γ-Fe_2O_3 by dehydration of γ-FeOOH are given below.

2.1. Seebeck voltage measurements

The sample in the form of a pellet of 10 mm thickness was pressed between two platinum disks fixed at the ends of two ceramic blocks. One of these blocks was spring-loaded to obtain good pressure contact. This sample holder along with the sample was placed in a constant temperature zone of a furnace, whose temperature was held to within ± 1° C. The temperature of the ends of the sample were measured with Chromel–Alumel thermocouples, placed in such a way as to touch the sample ends. These junctions were insulated from the platinum disks and ceramic block by means of thin mica sheets.

0022–2461/82/092503–11$03.82/0

During the measurements, the sample was equilibrated at each temperature for about 10 to 15 min. Temperature differences of 2 to 20° C were used along the sample. The thermoelectric voltage (or Seebeck voltage) developed across the sample and the temperature of the sample ends were read on a Philips PP 9004 microvoltmeter. A set of the values of thermoelectric voltage at various temperatures thus obtained ($\mu V K^{-1}$) was plotted against the respective absolute temperatures. The predominant charge carriers in a temperature gradient diffuse towards the cold end of the sample. The sign of the probe at the lower temperature is the sign of the Seebeck voltage.

2.2. Preparation of γ-Fe_2O_3 by dehydration of γ-FeOOH

Gamma-FeOOH was prepared [2] by hydrolysing $FeCl_2$ solution with an aqueous ammonia, and oxidizing with oxygen from the air. One hundred and fifty ml $FeCl_2$ solution (0.025 M) was mixed with 100 ml ammonia/ammonium chloride (0.1 M) and air was introduced into the mixture at a rate of 500 ml min^{-1} at 50° C. The temperature of the air was adjusted by using a water bath. The hydrogen ion concentration of the solution was maintained at pH 6.00 ± 0.02 by adding NH_4OH (0.1 M) from a burette. The pH of the mixture was measured continuously during the reaction using a glass electrode. An addition of about 130 ml NH_4OH (0.1 M) over 2 h was required for the completion of the reaction. The supernatant was tested with *o*-phenanthroline (1 % in ethanol) to guarantee the completion of the reaction. The suspension was then filtered, washed with a large quantity of water and dried at 60° C in an air oven yielding γ-FeOOH. The dried sample of γ-FeOOH was heated at 250° ± 1° C for one hour, yielding γ-Fe_2O_3.

The apparent densities of γ-Fe_2O_3 prepared from γ-FeOOH and $FeC_2O_4 \cdot 2H_2O$ are found to be 4860 kg m^{-3} and 4880 kg m^{-3} respectively (cf. 4790 kg m^{-3} in [3]).

3. Results and discussion

The log σ against T^{-1} (K^{-1}) plot (Curve I, Fig. 1) of a freshly prepared γ-Fe_2O_3 from $FeC_2O_4 \cdot 2H_2O$ shows an increase in electrical conductivity from room temperature (27° C) up to 140° C (Region A). Conductivity then decreases up to 217° C (Region B). A further increase in temperature increases σ (Region C) until the sample

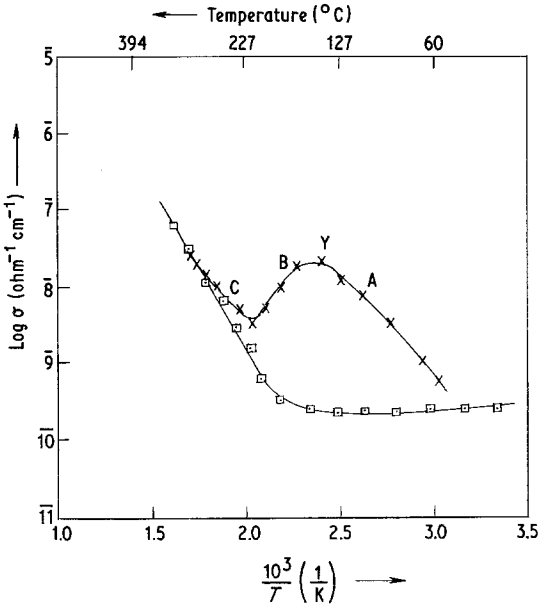

Figure 1 Plot of log σ against T^{-1} of freshly prepared γ-Fe_2O_3 from $FeC_2O_4 \cdot 2H_2O$ in static air. Curve I, X heating curve; II, ⊡ cooling curve.

transforms to α-Fe_2O_3 (at about 380° C). The electrical conductivity of γ-Fe_2O_3 heated at 315° C for 20 min decreases on cooling, and almost follows the extrapolation of Region C of the heating curve up to 185° C; during cooling the Regions B and A of the heating curve are not retraced; σ does not show any observable variation between 185° C and room temperature (Curve II, Fig. 1).

The nature of log σ against T^{-1} plot of γ-Fe_2O_3 stored for different times under static air is similar; however, the temperature ranges of Regions A and B are shifted to lower temperatures and a definite kink is observed in Region C of the curve. For example, a sample of γ-Fe_2O_3 stored under static air (r.h. 60%) for more than 7 days (Sample III) shows an increase in σ (Curve III, Fig. 2) in the temperature range 27° C to 60° C (Region A′), followed by a decrease in the temperature range 60° C to 100° C (Region B′). A further increase in temperature shows an increase in σ with a definite kink, k, at 177° C.

For the determination of the factors responsible for the observed maximum, Y′, and a kink, k, in the log σ against T^{-1} curve of γ-Fe_2O_3, the σ measurements were made using different atmospheres.

The σ of γ-Fe_2O_3 heated in dry nitrogen (Sample IV) at 300° C for 4 h shows a continuous decrease during cooling up to 180° C (Curve IV,

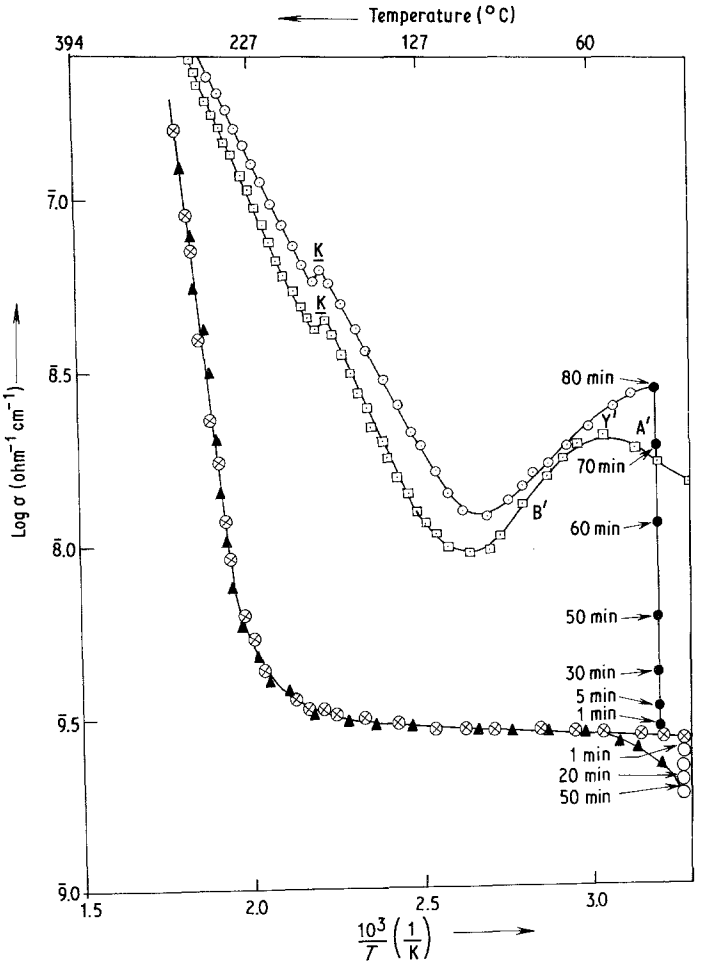

Figure 2 Plot of log σ against T^{-1} of γ-Fe_2O_3 equilibrated in static air. Curve III, ⊡ heating curve in static air (Sample III); IV, ⊗ cooling curve in dry nitrogen atmosphere (Sample IV); V, • Sample IV, equilibrated in $N_2 + H_2O$ at 40° C; VI, ⊙ heating curve of Sample V in dry nitrogen atmosphere; VIII, ○ Sample IV, equilibrated in $N_2 + O_2$, at room temperature; VIII, ▲ heating curve of Sample VII in N_2 atmosphere.

Fig. 2). It then remains practically constant up to room temperature. The heating curve of this sample in dry nitrogen overlaps Curve IV. No kink corresponding to k or a maximum corresponding to Y′ is noted. These observations indicate that the Regions A′, B′ and the kink k of Curve III (Fig. 2) are the characteristics of a sample of γ-Fe_2O_3 equilibrated with static air.

The differential thermal analysis (DTA) curve of Sample III displays two exothermic peaks at 170 and 405° C and a hump at 100° C. A careful analysis of the thermogravimetric (TG) curve shows about 1.2% loss up to 100° C and 0.8% loss between 100 and 180° C. The exotherm observed at 100° C corresponds to the desorption of water from the particle surface, and the exotherm observed at 170° C is probably associated with the decomposition of the hydrogen ferrite phase. The exotherm observed at 405° C is associated with the transformation of metastable γ-Fe_2O_3 to α-Fe_2O_3. It is interesting to note that the DTA curve of Sample IV does not show any clear exothermic peak up to 500° C.

It is known that adsorbed gases from the atmosphere, such as O_2 and H_2O, affect electrical conductivity [4–6]. To analyse the effect of these constituents a sample heated in dry nitrogen for 4 h and cooled and stored in the same atmosphere (Sample IV) was used. The σ measurements of Sample IV were carried out in the following atmospheres; (i) $N_2 + H_2O$, (ii) $N_2 + O_2$, (iii) H_2. The experimental results are shown in Figs 2 and 3.

The experimental set-up used for preparing the $N_2 + H_2O$ atmosphere did not allow us to take the measurements below 40° C. The σ of Sample IV was $4.6 \times 10^{-9}\,\Omega^{-1}\,cm^{-1}$ in N_2 at 40° C, and it steadily increases to $4.5 \times 10^{-8}\,\Omega^{-1}\,cm^{-1}$ within 80 min in $N_2 + H_2O$ (Curve V, Fig. 2). This equilibrated sample showed a decrease in σ up to 100° C in dry nitrogen, followed by an increase with a kink at 175° C (CurveVI, Fig. 2).

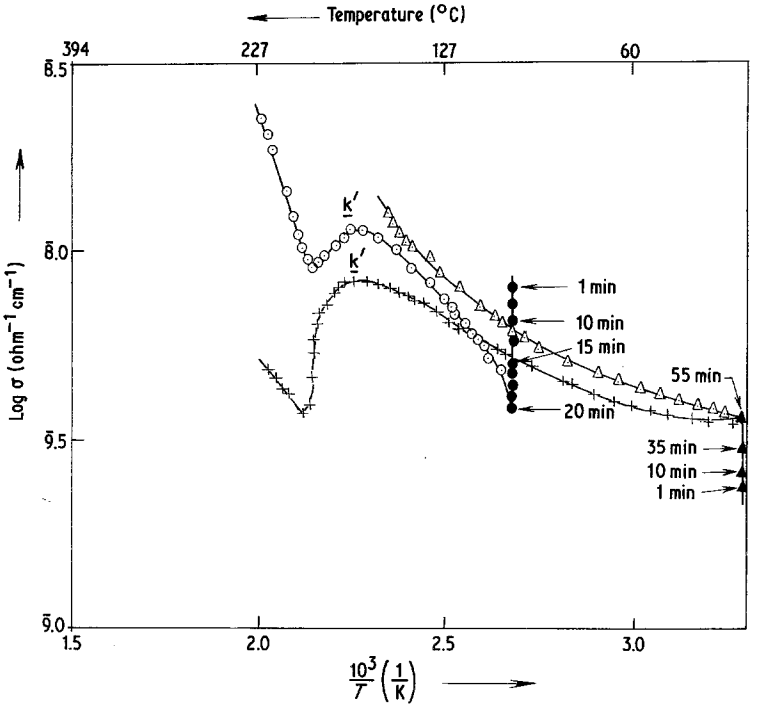

Figure 3 Plot of log σ against T^{-1} of γ-Fe_2O_3 in the different atmospheres. Curves IX, • Sample III equilibrated at 100° C in static air; X, ⊙ heating curve of Sample IX in N_2 atmosphere; XI, ▲ Sample IV equilibrated in H_2 atmosphere at room temperature; XII, ◬ heating curve of Sample XI in H_2 atmosphere; XIII, + heating curve of Sample XII in N_2 atmosphere.

When Sample IV was exposed at room temperature (27° C) to $N_2 + O_2$ atmosphere, the conductivity value decreased from 3.8×10^{-9} Ω^{-1} cm^{-1} with time, and remained constant after 50 min at $2.6 \times 10^{-1}\,\Omega^{-9}\,cm^{-1}$ (Curve VII, Fig. 2). In the N_2 atmosphere the σ of Sample VII increased on increasing temperature up to 60° C, and above 60° C, it practically overlapped the σ values of Sample IV (Curve VIII, Fig. 2).

These observations suggest that (i) an increase in σ of Sample IV when exposed to $N_2 + H_2O$ atmosphere is due to the adsorption of water on γ-Fe_2O_3; a decrease of σ in this equilibrated sample on heating is due to the desorption of water; (ii) a decrease in σ of Sample IV when exposed to $N_2 + O_2$ atmosphere is due to the adsorption of O_2 on γ-Fe_2O_3; a slow increase in σ on heating up to 60° C is due to the desorption of oxygen. Usually the adsorbed water behaves as an electron donor, and the adsorbed oxygen behaves as an electron acceptor [6–8]. Thus, Region A′ in the electrical conductivity curve of Sample III (Curve III, Fig. 2) corresponds to the desorption of oxygen, and Region B′ corresponds to the desorption of H_2O.

Sample VII heated in N_2 atmosphere did not show a kink, k, in the log σ against T^{-1} curve (Curve VIII, Fig. 2). This kink is clearly seen in the heating curve of a sample equilibrated in $N_2 + H_2O$ (Curve VI, Fig. 2). It may be noted here that the data of log σ against T^{-1} curve presented in Fig. 2 was determined using the heating rate 3° C min^{-1}. To distinguish more clearly the kink, k is would be advisable to desorb completely the adsorbed oxygen and water by equilibrating it at 100° C. The use of a dry atmosphere for the σ measurements of an equilibrated sample would further enhance the resolution of the kink, k.

Sample III was equilibrated at 100° C in static air (r.h. 60%) until σ remains constant. It required about 20 min (Curve IX, Fig. 3). At this stage, dry nitrogen was passed over the sample and the σ measurements were carried out at different temperatures (Curve X, Fig. 3). The kink k' is more prominently seen in Curve X. This observation suggests that H_2O is held in γ-Fe_2O_3 by two different types of forces. The physically adsorbed water on the upper surface of the particles of γ-Fe_2O_3 is removed up to 100° C. It is accompanied with a decrease in the σ. Some of the water molecules are held by lattice forces. It is possible that γ-Fe_2O_3 participates in hydrogen bonding with lattice water. An increase in σ with an increase in temperature of this sample suggest that some electron acceptor has been accommodated in the lattice in the temperature range 100 to 170° C. Here we tentatively assume that the lattice water cannot be removed without decomposition into

oxygen and hydrogen. Under these conditions, oxygen is desorbed as oxygen molecules, while hydrogen remains in the lattice due to the strong lattice forces. The observed kink k' will therefore be associated with the presence of hydrogen accommodated in the lattice. Such a mechanism can explain the probable origin of the hydrogen ferrite phase. It is reported in the literature that γ-Fe_2O_3 contains as much as 18.5 wt% adsorbed water, and as much as 0.16 wt% hydrogen [3, 9]. To substantiate the presence of hydrogen ferrite phase, the σ measurement of Sample IV in an H_2 atmosphere will be helpful.

When Sample IV is exposed to H_2 atmosphere at room temperature a constant electrical conductivity measurement is obtained after 55 min (Curve IX, Fig. 3). During this time the σ increases from $3.8 \times 10^{-9}\ \Omega^{-1}\ cm^{-1}$ to $5.7 \times 10^{-9}\ \Omega^{-1}\ cm^{-1}$. The temperature variation of electrical conductivity of this equilibrated sample in H_2 is represented by Curve XII (Fig. 3). A continuous increase in σ is observed in the heating curve. For the electrical conductivity measurements in H_2 atmosphere, temperatures lower than 150° C are used to avoid the reduction of γ-Fe_2O_3 to Fe_3O_4 [10, 11]. The conductivity measurements at higher temperatures of such a sample are therefore determined in N_2 atmosphere (Curve XIII, Fig. 3). A well-reserved characteristic maximum k' in σ is observed at 170° C. This maximum in the curve corresponds to the kink, k, observed for Sample III in static air, and for Sample IV in the $N_2 + H_2O$ atmosphere. It should be noted here that the kink, k', is also well resolved in Curve X (Fig. 3). These observations suggest the presence of the hydrogen ferrite phase.

The temperature corresponding to the interception of the tangents drawn at the inflection point in Curve IV (Fig. 2) is 225° C. This temperature is higher than the temperature at which the kink, k, is observed. Above 225° C the Curves IV (Fig. 2) and XIII (Fig. 3) practically overlap. However, the Curves III, VI (Fig. 2) and X (Fig. 3) overlap with Curve IV (Fig. 2) only above 280° C. Thus Sample III or Sample IV exposed to H_2O do contain electron acceptors even after the observation of the kink, k. The infra-red spectra of γ-Fe_2O_3 suggest that Sample III does contain water molecules up to 280° C. It may be assumed from the σ measurements and infra-red spectra that the sample heated at 280° C in N_2 for a long time (20 h) does not contain any water molecules. In Sample III some of the water molecules are removed at 100° C; above this temperature some of the water molecules decompose into hydrogen and oxygen. Hydrogen is trapped in the γ-Fe_2O_3 lattice. At 175° C the loss of hydrogen, and of a further amount of water takes place. We are tempted to suggest that the kink, k (or k'), corresponds to the beginning of the decomposition of hydrogen ferrite. Since Sample III and Sample IV display a similar behaviour of σ above 280° C, it is deduced that these two samples do not contain any lattice water or hydrogen above this temperature. Thus the hydrogen ferrite phase prevails mainly in the temperature range 100 to 280° C with a possible phase change at the kink, k. The hydrogen ferrite phase may also prevail below 100° C; it could not be detected by the σ measurements because between the room temperature and 100° C σ is mainly governed by the desorption of O_2 and H_2O. Since hydrogen remains in the lattice even in the high temperature range, one may cautiously assume that hydrogen occupies the vacancy sites in the spinel lattice. Thus the hydrogen ferrite will have a configuration similar to that of lithium ferrite. Once the hydrogen ferrite has formed, hydrogen cannot be desorbed merely by heating in the lower temperature range. The Sample IV obtained by heating γ-Fe_2O_3 in N_2 atmosphere for a long time probably does not contain any lattice water. It may be noted here that a sample of γ-Fe_2O_3 previously dried at 250° C in normal atmosphere contains 0.41% water, as has been determined by heating it in helium atmosphere at 950° C [9]. However, we have not observed any infra-red bands due to OH_2 for a sample heated in N_2 for a prolonged time at 280° C. It is likely that the strongly bound lattice water gives broad infra-red bands which could not be detected at low concentration.

The infra-red spectra of γ-Fe_2O_3 under the different experimental conditions show interesting results. The bands associated with the lattice water molecules are broad and are observed at 3400(s)* and 1650(s) cm^{-1}. The simulation presence of these two bands excludes the possibility of the presence of a detectable amount of OH^- [12]. In addition to these two bands, comparatively weak but much less broad bands are observed at 2720 cm^{-1}

*s = strong.

TABLE I Infra-red spectra of γ-Fe_2O_3 *

Sample	ν_{Fe-O} (cm^{-1} ± 2)
1. Stored under static air.	687(s), 634(s) 548(s), 365(s)
2. Heated at 110° C in static air, and cooled and stored under nitrogen	694(s), 643(s), 564(s), 370(s)
3. Heated at 280° C in a nitrogen atmosphere and cooled and stored under nitrogen (Sample IV)	694(s), 639(s), 550(s), 370(s),
4. Heated at 150° C in a hydrogen atmosphere, and cooled and stored under hydrogen (Sample XII)	694(s), 639(s), 550(s), 370(s)

*Infra-red spectra of γ-Fe_2O_3 prepared from $FeC_2O_4 \cdot 2H_2O$ and γ-FeOOH are similar to that of the standard sample.

and 2660 cm^{-1}. The intensities of these bands decrease on heating, and they disappear only after a prolonged heating (> 20 h) at 280° C in N_2. More than seven bands are observed in the region 710 cm^{-1} to 370 cm^{-1} due to the metal–oxygen vibrational modes. Four out of these seven bands are sharp and are of strong intensity. It seems that the positions of these bands depend on the history of the sample (Table I). The infra-red spectra of γ-Fe_2O_3 prepared from oxalate $FeC_2O_4 \cdot 2H_2O$, and γ-FeOOH have identical spectra, comparable with that of the standard. The sample heated at 110° C shows a blue shift for all the four bands. The band at 548 cm^{-1} has shifted to 564 cm^{-1} showing comparatively a high blue shift. It may be noted here that at 110° C the adsorbed O_2 and OH_2 are removed from γ-Fe_2O_3, as is observed from the electrical conductivity measurements. Another important feature of the spectra at 110° C is that bands are sharper as compared with that for Sample III. The infra-red spectra of a sample heated under N_2 atmosphere at 280° C (Sample IV) show some resemblance to that of a sample heated at 110° C under static air; for Sample IV the bands are much sharper and the band at 546 cm^{-1} shows a shift towards the lower energy (Table I). These changes are probably due to the removal of lattice OH_2 and hydrogen from γ-Fe_2O_3 at 280° C. In the literature [3] the effect of particle size on infra-red spectra, Mössbauer spectra and magnetic properties has been studied. The particle size of samples used in the present work lies in the range 93.0 nm to 95.0 nm in diameter, as has been determined from electron microphotographs. A comparison of the infra-red and Mössbauer spectra [13] determined in the present work with that reported in the literature also suggests that the particle size of our samples is large. For such samples the differences observed in the infra-red spectra are possibly due to the removal of adsorbed and lattice water, and may not be due to a small change in the particle size. It should be noted here that all the procedures used in the present work for making mulls required for infra-red were identical in each case.

The infra-red spectra and direct current electrical conductivity measurements of γ-Fe_2O_3 prepared from $FeC_2O_4 \cdot 2H_2O$ [1] and γ-FeOOH [2] show similar behaviour. However, the magnetic properties of γ-Fe_2O_3 prepared from γ-FeOOH and $FeC_2O_4 \cdot 2H_2O$ using static air are different (Table II). The saturation magnetization of a sample prepared from γ-FeOOH is much lower than that of a sample prepared from $FeC_2O_4 \cdot 2H_2O$. It is interesting to observe that the satu-

TABLE II Magnetic data of γ-Fe_2O_3

γ–Fe_2O_3	Coercive force (Hc) (A m^{-1})	Saturation magnetization (T kg^{-1})	Ratio remanence to saturation magnetization (M_R/M_S)
1. Prepared from $FeC_2O_4 \cdot 2H_2O$	3.14	7.10	0.64
2. Prepared from γ-FeOOH (Sample I)	3.52	6.15	0.65
3. Sample I heated at 280° C in a nitrogen atmosphere (Sample IV)	3.52	7.15	0.69
4. Sample I heated at 150° C in a hydrogen atmosphere (Sample XII)	3.52	7.06	0.67

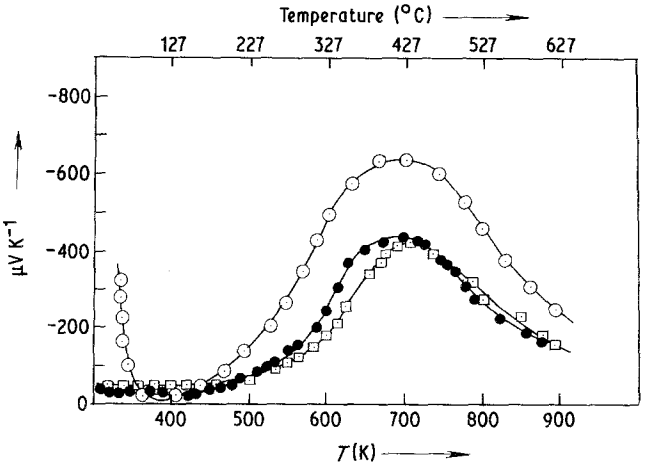

Figure 4 Plot of Seebeck voltage ($\mu V\ K^{-1}$) against T(K) of γ-Fe_2O_3. Curve XIV, ⊙ Sample III, static air; XV, ⊡ Sample IV, N_2, atmosphere; XVI, • Sample XII, N_2 atmosphere.

ration magnetization of a sample obtained from γ-FeOOH is greatly enhanced when the sample is heated in N_2 atmosphere at 280° C and brought to room temperature under N_2 atmosphere. Thus the structural details of two samples of γ-Fe_2O_3 prepared from two different starting materials, which could not be detected from the infra-red spectra, direct current electrical conductivity and X-ray diffraction patterns, are detected from the magnetic data. Since the magnetic properties are also comparable once the sample prepared from γ-FeOOH is heated in the nitrogen atmosphere, we are tempted to suggest that the surroundings of lattice water in Sample III of γ-Fe_2O_3 depend on the structural features of the starting compounds used for the preparation of γ-Fe_2O_3.

The activation energy determined from the log σ against T^{-1} curve of Sample IV under the nitrogen atmosphere is low (< 0.05 eV) in the temperature range 25 to 215° C. The carrier concentration is therefore constant in this region, and a small change in electrical conductivity with a change in temperature is due to the changes in the carrier mobility. During the cooling stage of the synthesis of γ-Fe_2O_3 the donors are frozen into the lattice. The Seebeck voltage of Sample IV is practically independent of temperature within experimental error between 25 and 215° C, and is of negative sign (Curve XV, Fig. 4). This observation indicates that the carriers are n-type and their number in this temperature range remains constant. In the temperature range 225 to 380° C the activation energy is as high as 0.95 eV. In this temperature range the negative Seebeck voltage increase with increasing temperature. Thus the concentration of the negative carriers is also changed in this temperature range. The Seebeck coefficient remains constant in the temperature range 395 to 445° C. In this temperature range the conductivity shows a weak but difinite inflection point, and γ-Fe_2O_3 transforms to α-Fe_2O_3. The negative carriers are possibly formed due to the loss of oxygen during the synthesis of γ-Fe_2O_3. Thus γ-Fe_2O_3 is possibly oxygen deficient. Some of the iron will therefore have to be in the oxidized state, + 2 [9]. The ferrous content was found to be between 0.24 to 0.62 (± 0.01) wt% in the different samples synthesized using identical experimental conditions.

Let us now analyse the data of Seebeck coefficient determined for Sample IV equilibrated with a hydrogen atmosphere at 150° C (Sample XII). The Seebeck voltage of Sample XII (Curve XVI, Fig. 4) does not show any observable change up to 170° C in a dry nitrogen atmosphere and is negative. Above 170° C the negative Seebeck voltage increases continuously up to 425° C, at which γ-Fe_2O_3 transforms to α-Fe_2O_3. From the log σ against T^{-1} curve for Sample XII in the dry nitrogen atmosphere the activation energy is low (< 0.05 eV) up to 65° C, and it increases to 0.11 eV in the temperature range 65 to 170° C.

When Sample IV is exposed to static air the activation energy is 0.38 eV in the temperature range 100 to 170° C, and is 0.44 eV after the inflection point, k. The temperature variation of Seebeck voltage for this sample is complex up to 100° C. Its value is least negative at 115° C, and the negative value increases with an increase in temperature above 115° C (Curve XIV, Fig. 4).

The results of the activation energy determined from the log σ against T^{-1} curve and of the temperature variation of Seebeck voltage suggest that the number of the negative carriers depends upon

the atmosphere. The nature of the carrier is not changed on changing the atmosphere. Under static air the number of carriers increases at comparatively lower temperatures than that under the nitrogen atmosphere. Thus the desorption of oxygen, water and possibly of hydrogen increases the number of negative carriers.

A hopping mechanism suggested for explaining the direct current electrical conductivity of ZnO can be used to explain the direct current electrical conductivity of γ-Fe_2O_3 [14, 15]. Such a mechanism is associated with a small value of activation energy. The small polaron can migrate by thermal activation from Fe^{2+} to Fe^{3+} leading to a change in mobility with a change in temperature [14, 16–18]. This mechanism requires the reduction of a small but definite fraction of Fe^{3+} to Fe^{2+} with a simultaneous removal of co-ordinated oxygen to satisfy the neutrality of a crystallite of γ-Fe_2O_3 as a whole.

The activation energy of the Sample IV in the nitrogen atmosphere above 225° C is much higher (0.95 eV) than that in the static air (0.44 eV). This observation suggests that the energy required for the removal of oxygen from γ-Fe_2O_3 in the nitrogen atmosphere is much higher than that in the static air. Thus the constituents of γ-Fe_2O_3 such as H_2O and hydrogen under static air, help the removal of oxygen from γ-Fe_2O_3. It is obvious that the polarization due to the lattice water will affect the electrostatic energy between Fe^{3+} and O^{2-}.

The structure of γ-Fe_2O_3 is usually represented as $Fe_8^{3+}\ [Fe_{40/3}^{3+}\ \square_{8/3}]\,O_{32}$ where $\square$ denotes a vacancy [19, 20]. The hydrogen present in γ-Fe_2O_3 will occupy some of the vacancy sites. Such γ-Fe_2O_3 will have a composition [9] between $Fe_8^{3+}\ [H_4^{1+}\ Fe_{12}^{3+}]\,O_{32}$ and $Fe_8^{3+}\ [(Fe_{4/3}^{3+}\ \square_{8/3})\ Fe_{12}^{3+}]\,O_{32}$. The composition of hydrogen ferrite, $Fe_8\,[H_4Fe_{12}]\,O_{32}$, corresponds to that of lithium ferrite $Fe_8\,[Li_4Fe_{12}]\,O_{32}$ [12, 21, 22]. These unit cell formulae suggest that the spinel structure, the lithium ferrite structure and the tetragonal γ-Fe_2O_3 structure are three different but related structure types in which the octahedral sites undergo a progressively greater degree of ordering. An intermediate composition $Fe_8[(Fe_x^{2+}H_{4-2x}\ \square_x)Fe_{12}^{3+}]\,O_{32}$ is also possible. Thus γ-Fe_2O_3 with an intermediate composition will contain Fe^{2+} which will also contribute to the proposed hopping mechanism of the direct electrical conductivity.

If the hydrogen ferrite (Sample XII) were a defininte phase with a cell constant sufficiently different from pure γ-Fe_2O_3 (Sample IV), the X-ray diffraction study would give an indication of these two phases. As already discussed in a previous paper, the X-ray diffraction pattern of Sample IV is sharp and corresponds to a tetragonal configuration [1]. The X-ray diffraction pattern of Sample XII is similar to that reported for the tetragonal γ-Fe_2O_3 [1], except that a definite hump on every component of the main pattern has been observed (Pattern c, Fig. 5). This observation suggests that Sample XII is a mixture of two compounds (Table III). We tentatively suggest that Sample XII is a mixture of hydrogen ferrite and γ-Fe_2O_3. The X-ray diffraction lines due to planes (220), (513) and (440) are well resolved. These patterns were fitted by an iterative method using the RESOLVE program [24] for a Gaussian shape of the two component lines. The values of a and c lattice parameters for the tetragonal structure of γ-Fe_2O_3 and hydrogen ferrite thus determined were used to calculate the positions of lines due to the reflections from other planes (Pattern d, Fig. 5). The calculated values were fitted with the experimental pattern by an iterative method giving the following final sets of lattice parameters:

γ-Fe_2O_3 $\quad a = 0.8355$ nm; $c = 2.500$ nm

Hydrogen ferrite $a = 0.8319$ nm; $c = 2.420$ nm

The a values of γ-Fe_2O_3 and hydrogen ferrite are comparable with the literature data for γ-Fe_2O_3 and lithium ferrite [12] respectively. The X-ray diffraction pattern of Sample IV, stored under static air for 7 days, shows comparatively broad bands (Pattern a, Fig. 5). It may be noted that the neutron diffraction pattern of γ-Fe_2O_3 reported in literature [25, 26] could not indicate the presence of the hydrogen ferrite phase; the sample used for this study was not however treated under hydrogen as we have done for obtaining the equilibrated sample. Another interesting observation is related to the relative intensities of the diffraction pattern associated with the planes (113), (400) and (226) which are assigned to the vacancy sites [20]. For Sample IV the relative intensities of lines due to these planes are much higher (Pattern b, Fig. 5), and the diffraction pattern in the high angle region is also clearly defined. For example the relative intensity of the (226) line for Sample IV is about twice

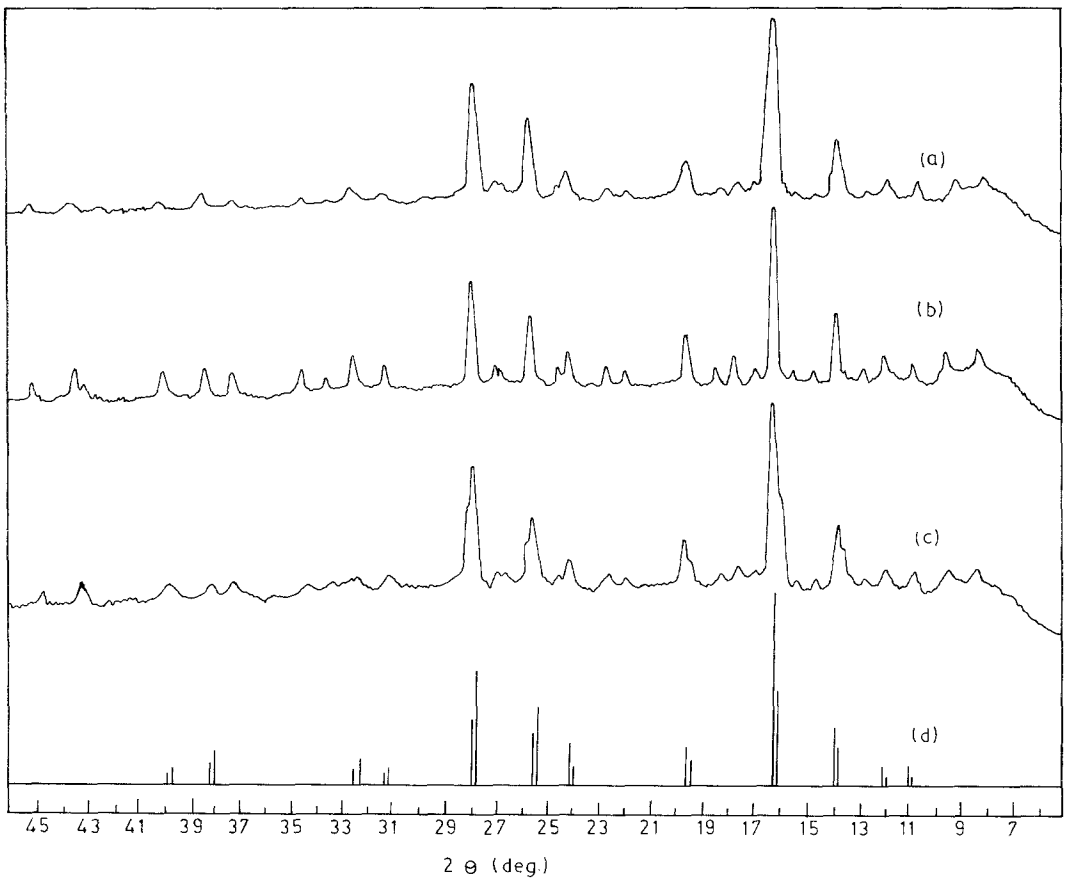

Figure 5 X-ray diffraction pattern of γ-Fe_2O_3. (a) stored under static air; (b) heated at 280° C in dry nitrogen atmosphere for 20 h and cooled and stored under nitrogen (Sample IV); (c) heated at 150° C in hydrogen atmosphere, cooled and stored under hydrogen (Sample XII); and (d) computer fitting of pattern (c).

that for Sample XII. The pattern in the high angle region for Sample XII is also comparatively diffuse.

The presence of water molecules in γ-Fe_2O_3 has been well documented [3, 9, 12, 20] and it has been suggested that the stability of the metastable phase is associated with these water molecules. The temperature variation of direct current electrical conductivity of γ-Fe_2O_3 in different atmospheres, infra-red spectra, and line width of X-ray diffraction pattern associated with the vacancy ordered lattice of differently treated samples have clearly indicated the presence of lattice water. It may be noted here that out of eight tetrahedral holes only one hole is occupied, and out of four octahedral holes only two holes are occupied in a one-eighth subcell of unit cell of spinel (the vacancy sites present in γ-Fe_2O_3 are in addition to these holes). We are therefore tempted to suggest that there is a sufficient space in a subunit cell to accommodate a water molecule, which will be strongly hydrogen bonded with the lattice oxygen.

The hydrogen ferrite phase can be considered to be the hydrogen-doped γ-Fe_2O_3. The data of σ at different temperatures of the doped samples of γ-Fe_2O_3 will be therefore useful in obtaining further insight into the proposed hydrogen ferrite phase. In particular the study of the effect of a dopant on the kink, k, in the log σ against T^{-1} curve will be interesting. The data of the Seebeck voltage of doped γ-Fe_2O_3 will also be useful to substantiate the proposed mechanism of the direct current electrical conductivity of γ-Fe_2O_3. This problem will be the subject of further work.

4. Conclusions

The curve log σ against T^{-1} for a freshly prepared sample of γ-Fe_2O_3 during the heating cycle does not overlap that determined during the cooling cycle. To analyse this observation the study of the direct electrical conductivity, σ, of γ-Fe_2O_3 has

TABLE III X-ray diffraction data of γ-Fe_2O_3

Lattice planes (*hkl*)	γ-Fe_2O_3 (tetragonal) *d*-spacing values [23] (nm)	Observed *d*-spacing values of γ-Fe_2O_3* (present study) (nm)	Observed *d*-spacing values of γ-Fe_2O_3 of Sample IV† (nm)	Observed *d*-spacing values of maximum intensity of Sample XII‡ (nm)	Computer fitted *d*-spacing values of Sample XII (nm)	
					γ-Fe_2O_3 $a = 0.8355$ $c = 2.500$	Hydrogen ferrite $a = 0.8319$ $c = 2.420$
101	0.791(1)	–	–	–	–	–
102	0.694(2)	–	–	–	–	–
110	0.590(6)	–	–	–	–	–
112	0.533(1)	0.5331(2)	0.5333(1)	0.5333(1)	–	–
113	0.482(6)	0.4819(5)	0.4820(6)	0.4819(6)	0.4820	0.4752
114	0.429(2)	0.4281(2)	0.4300(2)	0.4281(2)	–	–
210	0.373(6)	0.3732(5)	0.3731(5)	0.3739(6)	0.3738	0.3720
213	0.340(7)	0.3390(7)	0.3409(6)	0.3392(7)	0.3409	0.3378
214	0.320(3)	0.3205(3)	0.3205(3)	0.3205(3)	–	–
220	0.295(30)	0.2952(27)	0.2954(29)	0.2952(28)	0.2954	0.2941
300	0.278(3)	0.2790(2)	0.2789(3)	0.2780(3)	–	–
310	0.2683(4)	0.2645(3)	0.2638(4)	0.2640(4)	–	–
313	0.2514(100)	0.2516(100)	0.2517(100)	0.2516(100)	0.2519	0.2501
226	0.2408(2)	0.2398(2)	0.2408(4)	0.2403(2)	–	–
320	0.2315(2)	0.2329(4)	0.2315(5)	0.2316(2)	–	–
323	0.2230(2)	0.2231(2)	0.2231(2)	0.2229(2)	–	–
400	0.2086(15)	0.2083(16)	0.2089(17)	0.2083(15)	0.2089	0.2079
420	0.1865(1)	0.1863(1)	0.1863(1)	0.1863(1)	–	–
423	0.1820(3)	0.1819(4)	0.1825(3)	0.1820(3)	–	–
426	0.1701(19)	0.2691(18)	0.1795(19)	0.1691(19)	0.1705	0.1689
430	0.1670(2)	0.1670(2)	0.1670(2)	0.1669(2)	–	–
513	0.1604(20)	0.1594(21)	0.1606(20)	0.1600(20)	0.1608	0.1599
520	0.1550(2)	0.1550(2)	0.1550(2)	0.1550(2)	–	–
523	0.1525(3)	0.1519(4)	0.1525(3)	0.1519(3)	–	–
440	0.1474(40)	0.1471(38)	0.1476(40)	0.1476(40)	0.1476	0.1471
620	0.1318(6)	0.1314(7)	0.1318(6)	0.1318(6)	0.1321	0.1315
539	0.1272(8)	0.1267(8)	0.1274(10)	0.1271(8)	0.1274	0.1260
626	1.258(3)	0.1259(3)	0.1259(3)	0.1258(2)	–	–
442	0.1204(5)	0.1192(5)	0.1212(6)	0.1201(5)	–	–
646	0.1115(6)	0.1112(5)	0.1117(6)	0.1115(5)	0.1117	0.1109
733	0.1086(10)	0.1083(8)	0.1086(10)	0.1086(8)	0.1087	0.1083
800	0.1043(7)	0.1039(6)	0.1044(8)	0.1044(7)	0.1044	0.1039
826	0.0983(5)	0.0981(5)	0.0981(6)	0.0981(5)	–	–
753	0.0963(8)	0.0962(8)	0.0965(9)	0.0963(7)	0.0965	0.0960
840	0.0932(4)	0.0930(4)	0.0932(5)	0.0928(4)	–	–

*Stored under static air.
†Heated at 280° C in a nitrogen atmosphere, and cooled and stored under nitrogen (Sample IV).
‡Heated at 150° C in a hydrogen atmosphere, and cooled and stored under nitrogen (Sample XII).
The figures in brackets given in the table are intensities relative to the line width intensity (100).

been carried out in different atmospheres. This study has been supplemented with the data of infra-red spectra, magnetic properties and X-ray diffraction patterns of γ-Fe_2O_3 heated under different conditions. The important findings derived from this study are given below.

(a) The heating curve log σ against T^{-1} for γ-Fe_2O_3 stored in static air (Sample III) shows an increase in σ up to 60° C followed by decrease in σ up to 100° C. There is a further increase in σ with an increase in temperature up to 380° C at which γ-Fe_2O_3 transforms to α-Fe_2O_3. A kink, k, has been observed at 177° C.

(b) The study of σ in the different atmospheres suggests that the first increase in σ is due to the desorption of oxygen and the decrease following it is due to the desorption of water.

(c) The data of infra-red spectra and σ suggest that the adsorbed water in γ-Fe_2O_3 is present partly as the physically adsorbed water and partly as

lattice water. The presence of lattice water is shown up to 280° C.

(d) The physically adsorbed water is removed below 100° C. The removal of lattice water is accompanied with the decomposition of water. Some of the hydrogen formed during this decomposition takes up the vacancy sites.

(e) The kink, k, in the log σ against T^{-1} curve observed for a sample in static air at 177° C becomes more distinct after the complete removal of the physically adsorbed water (Sample X). This kink is thought to be associated with the hydrogen ferrite phase.

(f) The X-ray diffraction pattern of γ-Fe_2O_3 heated in a nitrogen atmosphere at 280° C and stored under nitrogen at room temperature displays sharp lines. The patterns for samples (i) equilibrated under hydrogen at 150° C, and (ii) Sample X heated at 170° C in the static air for 30 min and stored under nitrogen atmosphere, show a definite hump on every peak, suggesting the presence of two species with a similar crystal structure. The cell constants of these two species differ by a small value. This observation substantiates the suggestion of the presence of a hydrogen ferrite phase.

(g) The sign of the Seebeck voltage of γ-Fe_2O_3 is negative in the temperature range 27 to 380° C. The nature of the temperature variation of Seebeck voltage resembles the temperature variation of the direct current electrical conductivity. In the nitrogen atmosphere it is small up to 225° C. At 225° C a sharp increase in the negative Seebeck voltage is observed, and it shows a small change with a further increase in temperature above 380° C (up to 445° C). A hopping mechanism involving the negative charge carriers has been used to explain these results.

(h) The magnetic properties of γ-Fe_2O_3 synthesized from γ-FeOOH are different (6.14 T kg^{-1}) from those of a sample prepared from $FeC_2O_4 \cdot 2H_2O$ (7.10 T kg^{-1}). When the former sample is heated under the nitrogen atmosphere at 280° C for 20 h, the magnetic properties show an enhancement, and compare well with those of the latter sample.

Acknowledgements

This work has been undertaken with the financial support from Khosla Research Project. A senior fellowship (KSR) and a junior fellowship (AKN) have been awarded. Our thanks are due to the late Professor A. B. Biswas, Indian Institute of Technology, Bombay, India, for the facilities given for part of the work.

References

1. K. S. RANE, A. K. NIKUMBH and A. J. MUKHEDKAR, *J. Mater. Sci.* **16** (1981) 2387.
2. R. GIOVANOLI and R. BRÜTSCH, *Chimia* **28** (1974) 188.
3. J. M. D. COEY and D. KHALAFALLA, *Phys. Stat. Sol. (a)* **11** (1972) 229.
4. G. Y. ONODA Jr. and P. L. DeBRUYN, *Surface Sci.* **4** (1966) 48.
5. R. FURUICHI, N. SATO and G. OKAMOTO, *Bull. Chem. Soc. Japan* **42** (1969) 2475.
6. R. FURUICHI, N. SATO and G. OKAMOTO, *Chem. Abstracts* **73** (1970) 60193.
7. W. MEYER, *Z. Physik.* **38** (1937) 1014.
8. F. A. KROGER, "The Chemistry of Imperfect Crystals" (North Holland Publishing Co., Amsterdam, 1964) p. 475.
9. A. AHARONI, E. H. FREI and M. SCHIEBER, *J. Phys. Chem. Solids* **23** (1962) 545.
10. A. KPJIMA, *Sci. Rep. Res. Inst. Tohou Univ.* **A6** (1954) 178.
11. T. MASATAMI and H. SHUICHI, *Chem. Abstracts* **85** (1976) 136297.
12. I. DAVID and A. J. E. WELCH, *Trans. Faraday Soc.* **52** (1956) 1642.
13. A. K. NIKUMBH, Ph.D. Thesis, Poona University (1982).
14. I. G. AUSTIN and N. F. MOTT, *Adv. Phys.* **18** (1969) 41.
15. H. TAKEI and S. CHIBA, *J. Phys. Soc. Japan* **21** (1966) 1255.
16. J. YAMASHITA and T. KUROSAWA, *ibid.* **15** (1960) 802.
17. N. F. MOTT, *J. Non-Cryst. Solids* **1** (1968) 1.
18. I. G. AUSTIN, *ibid.* **2** (1970) 474.
19. E. J. W. VERWEY, *Z. Kristallogr.* **A91** (1935) 5.
20. K. P. SINHA and A. P. B. SINHA, *Z. Anorg. Chem.* **293** (1957) 228.
21. P. B. BRAUN, *Nature, London* **170** (1952) 1123.
22. E. W. GORTER, *J. Phys. Radium* **12** (1951) 189.
23. ASTM File number 25-1402.
24. G. BEECH, "Fortran IV in Chemistry: An introduction to computer-assisted methods", (John Wiley and Sons Ltd., New York, 1975) p. 142.
25. G. A. FERGUSSON and M. HASS, *Phys. Rev.* **112** (1958) 1130.
26. R. UEDA and K. HASEGAWA, *J. Phys. Soc. Japan.* **17** (Suppl. BII) (1962) 391.

Received 4 September 1981
and accepted 26 January 1982